

Three-dimensional finite difference modeling of static soil-pile interactions to calculate p - y curves in pile-supported slopes

Hasan Sharafi¹ · Yazdan Shams Maleki² · Mehran Karimpour Fard³

Received: 13 May 2014 / Accepted: 10 September 2015 / Published online: 8 December 2015
© Saudi Society for Geosciences 2015

Abstract In this paper, the slope effects on p - y curves in c - ϕ soils have been investigated. Vertical mono-pile under static lateral loading in level and sloped grounds with both cohesion and friction properties has been analyzed. Several concrete and steel pipe piles near soil slopes and level ground have been modeled. The basis of the numerical analysis is 3-D explicit finite difference method. The effects of pile-soil interface properties such as cohesion ratio and friction ratio on the soil response and pile deflections have also been investigated. The results of this research show that the general shape of p - y curves for c - ϕ soils and non-cohesive, granular soils are hyperbolic similar to p - y curves for clayey cohesive soils. This study that presents a new method and new design curves similar to concepts have been proposed by Evans and Duncan for derivation of ultimate soil strength, p_u , for piles in c - ϕ soils. There are a few numerical and experimental studies about piles under lateral loading in c - ϕ soils, and present study focuses on this shortcoming.

Keywords Vertical pile · Slope's effects · c - ϕ soils · p - y curves · Static analysis · Interface

✉ Mehran Karimpour Fard
mehran.karimpour@guilan.ac.ir

¹ Department of Civil Engineering, School of Engineering, Razi University, Kermanshah, Iran

² Razi University, Kermanshah, Iran

³ Department of Civil Engineering, Faculty of Engineering, University of Guilan, Guilan, Iran

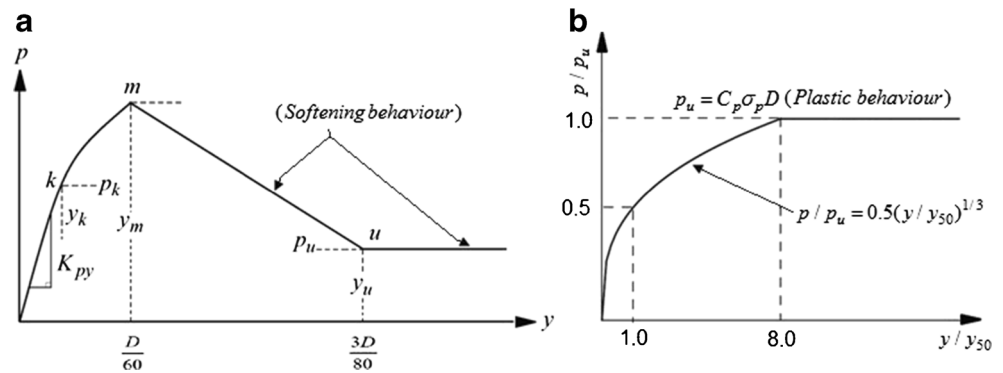
Introduction

Vertical mono-piles under static lateral loading are important cases of deep foundations. There are several loading cases in the piles subjected to static lateral loading such as the piles near natural or man-made slopes for bridge abutment foundations or as retaining walls, piles near slopes carrying lateral loads from power towers or wind turbines, foundation of traffic signs, piles for stabilizing slopes, piles for foundation of high-rise buildings near slopes, etc. Many researchers have studied the lateral load transfer curves (i.e., p - y curves) for many cases including loading conditions, soil types, geometry conditions (level ground or sloped ground), pore water pressure conditions in soil (undrained or drained soils), and many other different conditions.

Matlock (Matlock 1970) developed p - y curves for undrained soft clay, Reese et al. (Reese et al. 1975) introduced a series of p - y curves for stiff clay with free water, and Welch and Reese (Welch and Reese 1972) and Reese and Welch (Reese and Welch 1975) also developed stiff clay with no free water p - y curves. Reese et al. (Reese et al. 1974) developed sand p - y curves, and API (American Petroleum Institute 1987) introduced also sand p - y curves. Ismael (Ismael 1990) developed cemented sand p - y curves (see Fig. 1b), and after him, Reese and Van Impe (Reese and Van Impe 2001) developed silt p - y curves (Fig. 1a). For piles near or on slopes under lateral loading, there are a few studies in the related literatures. Reese et al. (Reese et al. 1975) proposed equations according to the passive wedge failure or flow failure for piles in sandy slopes and also p - y curves for piles in clayey slopes.

Furthermore, Georgiadis and Georgiadis (Georgiadis and Georgiadis 2010; Georgiadis and Georgiadis 2012) conducted a 3D finite element analysis for prediction of behavior of piles

Fig. 1 Characteristic shape of p - y curves proposed for c - ϕ soil by **a** Reese and Van Impe p - y curves for static horizontal lateral loading (Reese and Van Impe 2001) and **b** Ismael (Ismael 1990) p - y curve for cemented sand



near undrained clayey slopes. They have studied the effects of slope inclination, θ ; pile-soil interface adhesion factor, α ; and distance between pile cross section center and slope crest, b , on p - y curve behavior and lateral bearing capacity of concrete vertical mono-piles. Nimityongskul et al. (Nimityongskul and Ashford 2010; Nimityongskul et al. 2012) reported a research about effects of soil slope on lateral bearing capacity of piles in both cohesive and non-cohesive soils. They (Nimityongskul and Ashford 2010; Nimityongskul et al. 2012) also conducted a 3D finite element analysis in the PLAXIS 3D FOUNDATION software to comparing test results with numerical results.

Available studies about the lateral loading capacity behavior of piles in sloped ground are rare, and even these few ones basically refer to piles in non-cohesive (i.e., frictional) materials (Gabr and Borden 1990; Mezazigh and Levacher 1998; Zhang et al. 2004; Muthukkumaran et al. 2008).

The aim of this paper is to propose a method to calculate the bearing capacity of vertical mono-piles near sloped and level grounds consisting of c - ϕ soil based on the numerical analysis of three-dimensional finite difference analysis (3D FDA). Coulomb shear-strength criterion is used to define the material behavior of pile-soil interface considering some parameters such as cohesion, angle of internal friction, and dilation angle for the interfacial material. In order to define the pile-soil interfacial materials, Papadopoulou and Comodromos (Comodromos and Papadopoulou 2010) have used this criterion to evaluate the displacement amplification factor of R_a of pile groups in sandy soil; they (Comodromos and Papadopoulou 2013) have also used this criterion to evaluate the same factor in cohesive soils. Also, according to Papadopoulou and Comodromos (Comodromos and Papadopoulou 2010) and Comodromos and Papadopoulou (Comodromos and Papadopoulou 2013), the response of a pile group under lateral loading is of a similar form to that of a single pile. They investigated the variation of the deflection amplification factor, R_a , which is introduced when comparing the response of a pile group to that of a single pile (considering the same pile dimensions and soil profile). The R_a factor can be defined as the ratio of the group deflection at the pile cap

y_{mG} to the single-pile deflection at the pile head y_s , or as the ratio of the group normalized deflection y_{nG} to the single-pile normalized deflection y_{ns} , for the same mean load H_m . They have reduced the amount of internal friction angle of pile-soil interface material due to the critical state that has been listed by Ortigao (Ortigao 1995) compared to the angle of internal friction of the soil around the pile. On the other hand, cracking of soil around the pile and gap formation behind the pile during lateral loading are issues that have complicated the problem of piles under lateral loading numerical modeling.

The constitutive model of Coulomb shear-strength criterion for interface modeling is able to simulate some of these effects in piles under lateral loading. In this research, different slope inclinations and different distances between pile center and slope crest are taken into consideration. The pile-soil-pile interactions (PSPIs) have been modeled using pile-soil interface properties such as normal and shear stiffness of interface, cohesion, and internal friction angle of interface. The current paper, thus, investigates the effects of sloped ground on static lateral loading bearing capacity of vertical piles near the c - ϕ soil slopes. Present paper research about distinct effects of cohesion component and friction component of c - ϕ soils on p - y curves. The 3D explicit finite difference analyses were conducted to model first the lateral behavior of cohesion component of the soil and then for friction component of soil separately and finally for both cohesion and friction components of soil independently. After that, the obtained results presented together in a unit graphs were compared. Effects of cohesion and internal friction angle components of the c - ϕ soil (i.e., the decrease and increase in interfacial strength properties) have been investigated by parametric studies.

Problem definition and numerical approach

Problem methodology, hyperbolic p - y curves, and real pile-soil behavior

Initially, the equations that have been used by previous researchers (Matlock 1970; Reese and Welch 1975; Reese

et al. 1974) to create p - y curves at undrained clayey soils under the lateral loading were as follows:

$$p = 0.5p_u(y/y_{50})^n \tag{1}$$

$$y_{50} = C_1 d \varepsilon_{50} \tag{2}$$

where p_u is the ultimate load (kN/m) and y_{50} is the lateral deflection of pile at 50 % of the ultimate soil reaction (m). Moreover, C_1 is a constant relating pile deflection to laboratory strain ε_{50} , ε_{50} is the strain at 50 % of soil resistance equal to stress $(\sigma_1 - \sigma_3)_{\max}/2$ at triaxial tests, and σ_1 and σ_3 are the first and third principal stresses at triaxial tests (kN/m²), respectively. Besides, p is the soil reaction (kN/m), y is the pile deflection (m) corresponding to the p value, d is the pile diameter (m), and n is a constant relating soil resistance to pile deflection. As Eq. (1) gives an infinite initial curve slope in very small lateral deflections at low load levels (because $n < 1$), the hyperbolic curve (i.e., Eq. (3) below) has often been considered in describing of pile test results. According to the results of pile loading in soils and some rocks tests (Georgiadis and Georgiadis 2010; Georgiadis and Georgiadis 2012; Wu et al. 1998; Liang et al. 2009). the behaviors of almost p - y curves have a hyperbolic shape. Also, in current numerical analysis, this type of hyperbolic p - y curve was resulted as long as the elastic-plastic behaviors were used to soil material modeling and linear elastic model was used to pile materials. The hyperbolic curve has an initial stiffness as a slope K_i and is presented by the following equation (Liang et al. 2009; Georgiadis et al. 1991; Rajashree and Sitharam 2001; Kim et al. 2004):

$$p = \frac{y}{(1/K_i) + (y/p_u)} \tag{3}$$

where y is the lateral pile deflection (m), p is the soil reaction (i.e., load per unit length of the pile, kN/m), p_u is the ultimate soil reaction (kN/m), and K_i is the initial stiffness (slope) of p - y curves (kPa).

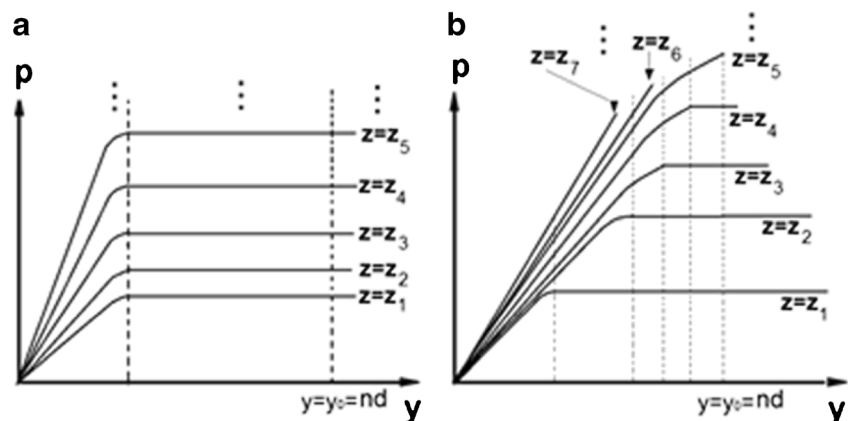
As the stress-strain behavior of soil is not linear (i.e., is completely non-linear), then considering such a non-linear equation to explain the interaction behavior of pile-soil seems

to be adequate. As observed in this case study, the behavior of p - y curve is hyperbolic for all types of soils including cohesive, frictional-granular, and mixed cohesive-frictional soils (i.e., the c - ϕ soils), and p - y hyperbolic curves are valid for a variety of soil conditions, including drained or undrained soils. In the present study, rather than focusing on K_i parameter, the p - y curve behavior in c - ϕ soils and the effects of soil cohesion and friction angle parameters are investigated. However, it is pointed out that both the symbols of d and D were used as the means of pile diameter in this research. This paper investigates the large-diameter (i.e., with diameters equal to 1 m in contrast with pile diameters that have been considered in lateral loading tests in Reese et al. (Reese and Van Impe 2007). mono-pile lateral loading bearing capacity behavior. Mono-piles are usually designed using the well-known p - y method. On the other hand, alternative design method that is the strain wedge method (SWM) has been developed by Norris (Norris 1986).

Lesny et al. (Lesny et al. 2007) by utilizing finite element analysis have shown that both methods (i.e., p - y curve method and SWM) overestimate the pile-soil stiffness of large-diameter mono-piles at great depths, which may result in an insufficient pile length design. These observations may be attributed to the linear distribution of the soil stiffness implied in these methods. This assumption leads to unrealistic pile-soil stiffness relations of large-diameter piles and therefore cannot properly reflect the pile response. Consequently, these methods should not be directly applied to large-diameter mono-piles.

There are two classes of pile-head deflections including (1) small pile-head deflections (e.g., $y = d/60$ or $y = 3d/80$ in ref. Reese and Van Impe (2007) and is given in Fig. 1a) and (2) large pile-head deflections. This paper investigates the large pile-head deflections, and the maximum pile-head deflection is considered 70 % of pile diameter (i.e., $y_{\max} = 0.7d$). In the theoretical literature, most attention has been paid on the small pile-head deflection behavior (Reese and Van Impe 2007) compared with large pile-head deflection behavior, and both pile-head load-deflection curves, H - y curves, and p - y curves

Fig. 2 Comparison between general shapes of p - y curves for short-term static horizontal loading for different depths below the ground surface: **a** theoretical (unrealistic idealized in previous numerical analysis) p - y curves and **b** real (experimental and 3D FDA in present study) p - y curves along the pile length for a particular pile-head deflection (in term of $n.d$) (Reese and Van Impe 2007)



have been derived for small pile-head deflections (see, e.g., Fig. 1).

In present study, the effects of ground water table has not been considered by authors and the soil medium is assumed as drained soil by the means that the long-term slope stability and principle of effective stresses have been considered. Further, in this study, it is tried to use true-type p - y curve fit to a specified pile displacement up to $y_0 = n \cdot d$ as shown in Fig. 2b. In other words, according to the previous numerical and theoretical studies (Reese and Van Impe 2007). for pile set displacement, the y_0 is considered up to 70 % of d ($n=0.7$), and the values of the ultimate strength of the soil p_u have been calculated at the different point along the pile length.

However, it should be noted that there is no any considerable lateral displacement of the piles that lead to interrupting for all soil layers in different depths (as shown in Fig. 2a). Since, the soil behavior represents that only the upper layers of the soil will be interrupted and cracked by lateral loading, and this is depending on soil characteristics for any specific pile displacement (as seen in Fig. 2b) and this practical reality is a base to practice in this research. It is pointed out that both numerical and experimental results for piles under static lateral loading show that the p - y curves at different depths do not have a similar behavior as parallel shapes (see Fig. 2a). As seen in Fig. 2a, p - y curve behaviors are very different in various depths, for example, in cohesive, granular, and mixed c - ϕ soils, and are remarkably variable depending on the type of stress distribution at the soil profile. However, it is mentioned that in the available literatures (Reese and Van Impe 2007). behavior of p - y curves in different depths along the pile axis is assumed parallel that it is not consistent with real pile-soil system behavior.

Literatures on p - y curves in sloped and level grounds for c - ϕ soils

Different relationships have been proposed to estimate the ultimate strength of the soil, p_{ult} in c - ϕ soil that generally separate the friction and cohesion effects of soil in estimating

Fig. 3 Geometry of problem including slope shape, pile location, lateral loading direction, and Cartesian coordinate system

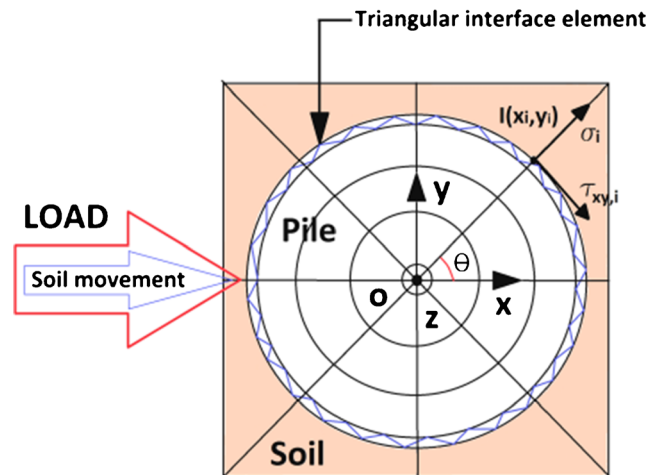
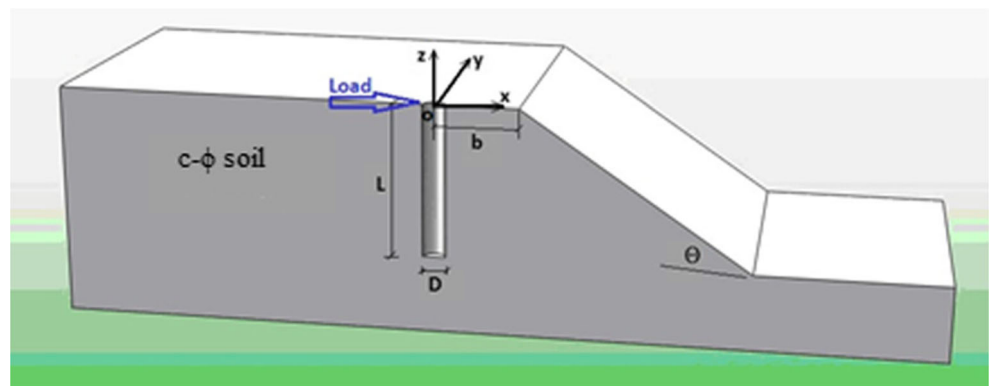


Fig. 4 Plan view of pile elements, soil elements, interface elements, center of pile-head coordinates (i.e., $x, y, z=0, 0, 0$), and vectors of interface normal and shear stresses

the ultimate capacity of the c - ϕ soil; the following equations are the most important equations of the present theory to calculate the ultimate strength of the c - ϕ soils. Evans and Duncan (Evans Jr and Duncan 1982) have recommended an approximate equation for calculation of ultimate resistance of c - ϕ soils for level ground (Reese and Van Impe 2007) as

$$p = \sigma_p d = C_p \sigma_h d \tag{4}$$

where σ_p is the passive earth pressure (kPa) including the three-dimensional effect of the passive wedge and d is the pile width or pile diameter (m) and

$$\sigma_h = \gamma z \tan^2 \left(45 + \frac{\phi}{2} \right) + 2c \tan \left(45 + \frac{\phi}{2} \right) \tag{5}$$

where σ_p is the Rankine's passive earth pressure (kPa) for a wall of infinite length, γ is the unit weight of soil (kN/m^3), z is the depth (m) at which the passive resistance is considered, ϕ is the friction angle (degree), c is the cohesion of soil (kPa), and C_p is a dimensionless modifying factor to account for the three-dimensional effect of the passive wedge failure (Reese and Van Impe 2007). The modifying factor C_p can be divided

Table 1 Summary of various pile’s lateral load tests in different kinds of soils

Pile test	Mechanical and geometrical characteristics						Soil properties				
	<i>L</i> (m)	<i>D</i> (m)	<i>E_pI_p</i> (kN m ²)	<i>e</i> (m)	<i>θ</i> (deg)	<i>t_w</i> (mm)	Soil ^a	<i>C</i> (or <i>C_u</i>) (kPa)	<i>E</i> (or <i>E₅₀</i>) (kPa)	<i>φ</i> (deg)	<i>γ</i> (or <i>γ'</i>) (kN/m ³)
1 Sabine	12.8	0.319	31280	0.305	0°	12.7	c ^a	14.4	2060	0	5.5
2 Lake Austin	12.8	0.319	31280	0.0635	0°	12.7	c ^a	32.25	2687.5	0	10
3 Garston	12.5	1.50	– ^b	0.900	0°	–	φ ^a	0	<i>N_{SPT}</i>	43, 37	–
4 Kuwait	5.0	0.30	20200	–	0°	–	<i>c-φ</i> ^a	20, 0	<i>N_{SPT}</i>	35, 43	17.90, 19.10
5 SCE pier (belled pier)	5.185 (17 ft)	1.22 (4 ft)	2.25×10 ⁶	0.230	20°	–	c ^a	220	24,440	0	18.85
6 SCE pier (belled pier)	6.710 (22 ft)	1.22 (4 ft)	2.25×10 ⁶	0.230	55°	–	c ^a	479	95,800	0	18.85

^a *C* cohesive soil, *φ* friction (non-cohesive) soil, *c-φ* cohesive-frictional soil

^b *E_pI_p* was not mentioned directly in ref. Reese and Van Impe (2007). and the cube strength of the concrete was 49.75 MPa

into the following two terms: *C_{pφ}* to modify the frictional term of Eq. (5) and *C_{pc}* to modify the cohesion term of Eq. (5) (Reese and Van Impe 2007). Equation (5) can then be written as (Reese and Van Impe 2007)

$$p_{ult} = \left[C_{p\phi} \gamma z \tan^2 \left(45 + \frac{\phi}{2} \right) + C_{pc} c \tan \left(45 + \frac{\phi}{2} \right) \right] d \quad (6)$$

The relative straightforwardness of equations for developing *p-y* curves for *c-φ* soil proceeds by using the concept proposed by Evans and Duncan (Evans Jr and Duncan 1982). Equation (6) will be written as (Reese and Van Impe 2007)

$$p_{ult} = \bar{A} p_{ult\phi} + p_{ultc} \quad (7)$$

where *A* (or *A*) can be found from the graph in ref. Reese and Van Impe (2007) and also in Figs. 17 and 18. Ultimate soil resistance for sand was derived by considering a wedge failure near the ground surface and a plane strain flow failure well below the ground surface as shown in Eqs. (8) and (9), respectively. The friction component (*p_{ultφ}*) for level ground will be the minimum of the values given by the Eqs. (8) and (9) as below:

$$p_{ult\phi} = \gamma z \left[\frac{K_0 z \tan \phi \sin \beta}{\tan(\beta - \phi) \cos \alpha} + \frac{\tan \beta}{\tan(\beta - \phi)} (d + z \tan \beta \tan \alpha) \right] + \gamma z [K_0 z \tan \beta (\tan \phi \sin \beta - \tan \alpha) - K_a d] \quad (8)$$

$$p_{ult\phi} = K_a d \gamma z (\tan^8 \beta - 1) + K_0 d \gamma z \tan \phi \tan^4 \beta \quad (9)$$

The cohesion component (*p_{ultc}*) for level ground will be the minimum of the values given by Eq. (11) as below:

$$N_p = 3 + \frac{\gamma'}{c} z + \frac{J}{d} z \leq 9 \quad (10)$$

$$p_{ultc} = \min \{ N_p c d, 9 c d \} \quad (11)$$

The lateral bearing capacity factor values, *N_p*, for cohesion component were obtained by placing the *p_u* values derived from 3D FDA of this research in Eq. (12) as follows:

$$p_{ultc} = N_p c d \quad (12)$$

where *K_a* = tan²(45 – φ/2) is the minimum coefficient of active lateral earth pressure; *z* is the depth of soil below the ground surface (m); *γ* and *γ'* are the total and submerge unit weights of soil (kN/m³), respectively; *d* is the pile diameter or

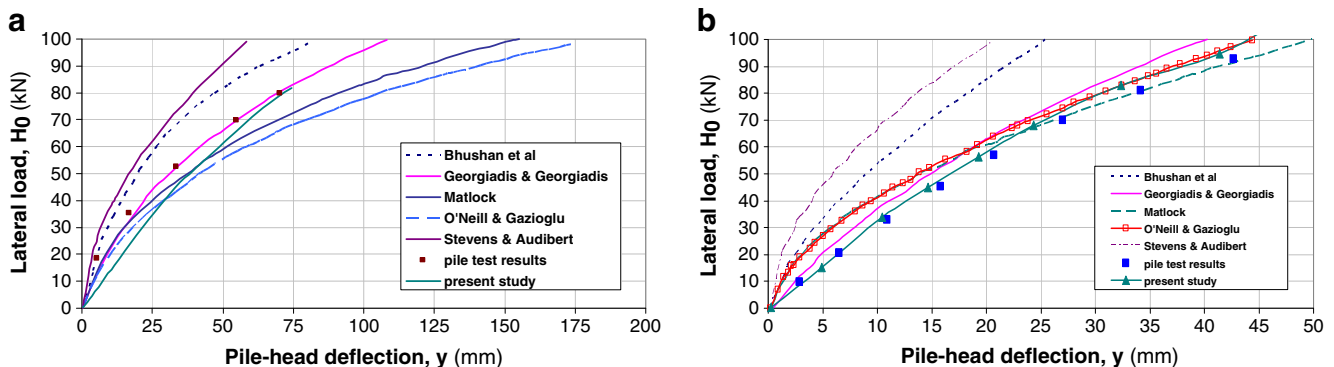


Fig. 5 Pile-head load-deflection curve for **a** Sabine River pile load test and **b** Lake Austin pile load test

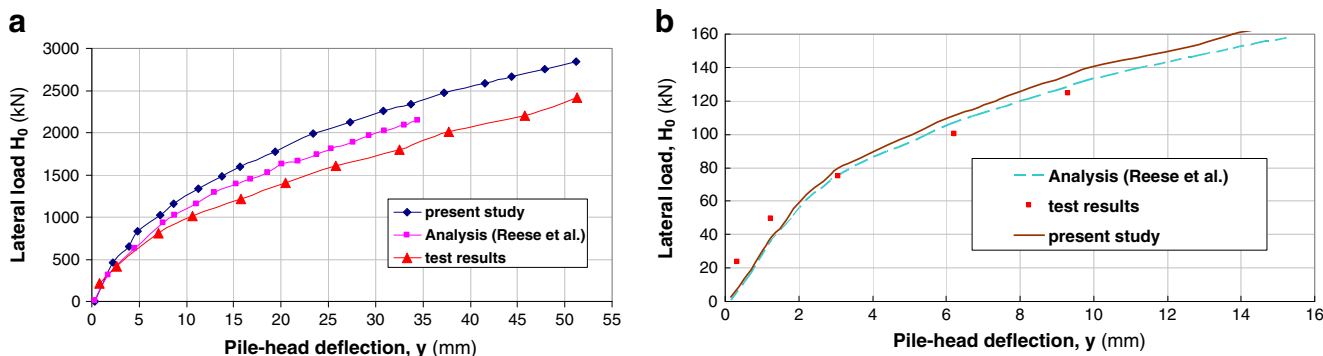


Fig. 6 Pile-head load-deflection curves for **a** Garston lateral load test results in non-cohesive soil (sand) and **b** Kuwait lateral load test in $c-\phi$ soil (cemented sands)

pile width (m), $\beta=45+\phi/2$ is the passive failure angle (degree); $\alpha=\phi/2$ is the angle defining the shape of the wedge (degree); and K_0 is an at-rest coefficient and it is equal to 0.4 and 0.5 for loose and dense sands, respectively. In a later study, Reese and Van Impe (Reese and Van Impe 2001) suggested the use of $K_0=0.4$ for all sands. In Eqs. (10)–(12), c is the cohesion of the soil (kPa) and J is a constant which controls the depth, and Matlock(Matlock 1970) stated the value of J to be 0.5 for a soft clay and about 0.25 for a medium clay. A value of 0.5 is frequently used for J . Reese and Welch (Reese and Welch 1975) considered the J equal to 0.5 for stiff clay, and Bhushan et al. (Bhushan et al. 1979) considered J equal to 2 for stiff clay. To develop the p versus y curves, the procedures described for sand by Reese et al. (Reese et al. 1974) will be used because the stress-strain behavior of $c-\phi$ soils is believed to be closer to that of non-cohesive soil than of cohesive soil (Reese and Van Impe 2007). This article uses a new approach similar to that in Eq. (7), with difference that it uses the results of 3D FDA numerical method to calculate the final strength value of soil, p_{ult} , in components of cohesion, friction, and both of those in combination (i.e., $c-\phi$ soil) and uses the following relationship:

$$p_{ultc\phi FDM} = Ap_{ult\phi FDM} + p_{ultc FDM} \tag{13}$$

where $p_{ultc\phi FDM}$, $p_{ult\phi FDM}$, and $p_{ultc FDM}$ are the stand for the ultimate resistance of the soil, for both cohesion and internal friction angle (i.e., $c-\phi$ soil), internal friction angle effect of the soil alone (i.e., granular soil), and soil cohesion alone (i.e., cohesive soil), respectively, derived from 3D FDA, and also A is a coefficient that resulted from Eq. (14) as the following:

$$A = \frac{p_{ultc\phi FDM} - p_{ultc FDM}}{p_{ult\phi FDM}} \tag{14}$$

The results of this study are presented in the following forms:

the graphs to calculate the coefficient A in order to calculate the ultimate soil resistance in $c-\phi$ soil, graphs to calculate the lateral bearing capacity factor N_p in order to calculate the ultimate strength of the cohesion component of $c-\phi$ soil in Eq. (7), and finally graphs for correction soil strength of the frictional component of $c-\phi$ soil in previous Eqs. (8) and (9). Overall, geometry form of the present study problem has been shown in Fig. 3.

Based on the results of the FE analyses that have been performed by Georgiadis and Georgiadis (Georgiadis and Georgiadis 2010; Georgiadis and Georgiadis 2012). the following equation was derived (similar to Murff and Hamilton’s equation (Murff and Hamilton 1993) for level ground and

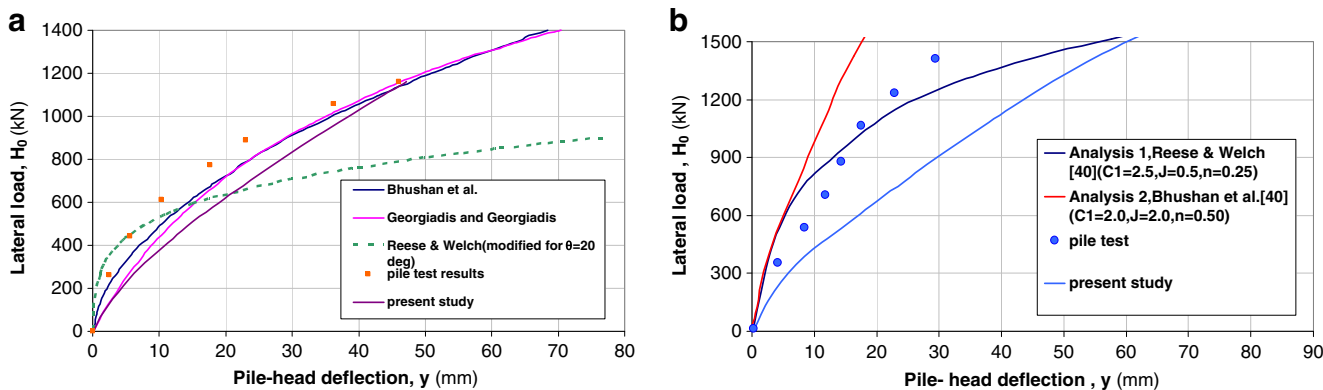
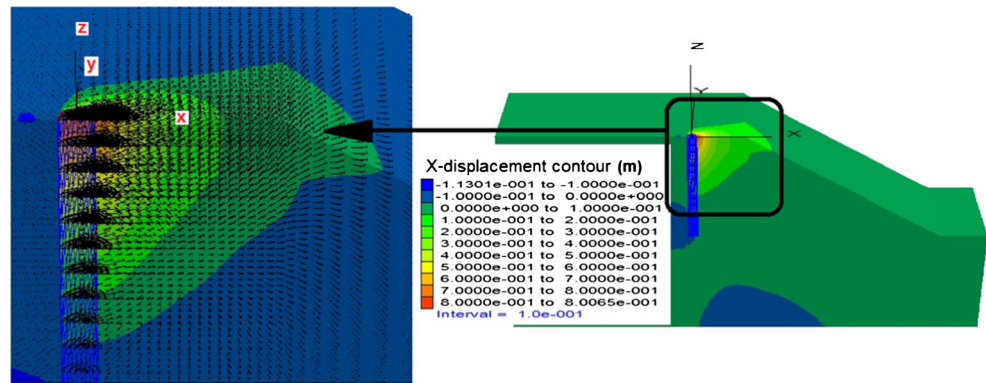


Fig. 7 Pier-head load-deflection curves for **a** Bhushan lateral load test results for $\theta=20^\circ$ slope in stiff silty clay (CL-CH) and **b** Bhushan lateral load test results for $\theta=55^\circ$ slope in cemented silty sand (SM)

Fig. 8 Contours of x displacement for $b=5.5d$, $L=12\text{ m}/d=1\text{ m}$, and $\theta=30^\circ$ and for horizontal loading along positive x direction ($y_{\max}=0.8d$ for ground surface) for $c-\phi$ soil and full interface strength ratio (length unit meter)



smooth piles), which approximates with good accuracy the variation of N_p factor with depth z for any value of ground inclination, θ , and adhesion factor, α

$$N_p = N_{pu} - (N_{pu} - N_{po} \cos \theta) e^{-\lambda(z/d)/(1+\tan \theta)} \tag{15}$$

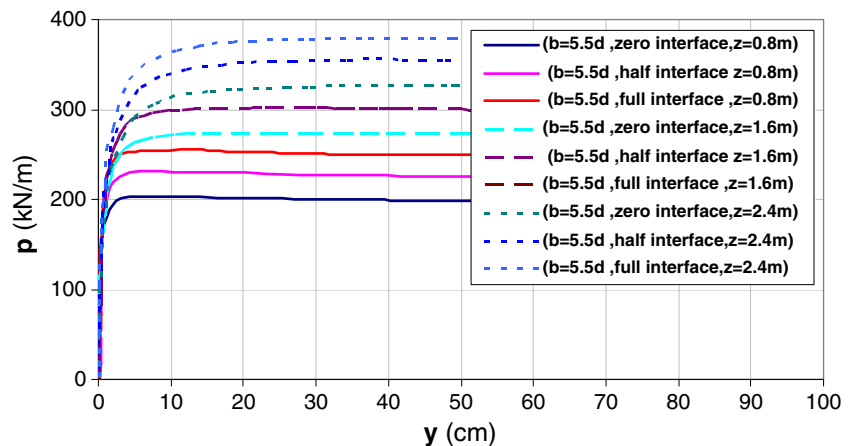
where N_{pu} is the ultimate lateral bearing capacity factor for deep lateral flow of soil (Eq. (17)), N_{po} is the bearing capacity factor at the surface for level ground, and λ is the dimensionless factor. This equation for level ground ($\theta=0^\circ$) reduce to

$$N_p = N_{pu} - (N_{pu} - N_{po}) e^{-\lambda(z/d)} \tag{16}$$

where the value of N_{po} varies linearly from 2 for a fully smooth ($\alpha=0$) to 3.5 for a fully rough ($\alpha=1$) pile-soil interface and given by $N_{po}=2+1.5\alpha$ and the value of the dimensionless factor λ also varies linearly with α from 0.55 for $\alpha=0$ to 0.4 for $\alpha=1$ and given by $\lambda=0.55-0.15\alpha$. The variation of N_p with z obtained with Eqs. (15) and (16) was compared to the FDA results in Figs. 16 and 17. Also, N_{pu} is the ultimate bearing capacity factor and (given by the two-dimensional lower bound plasticity solutions) was obtained by Randolph and Houlsby (Randolph and Houlsby 1984):

$$N_{pu} = \pi + 2\Delta + 2\cos\Delta + 4 \left(\cos \frac{\Delta}{2} + \sin \frac{\Delta}{2} \right) \tag{17}$$

Fig. 9 Hyperbolic p - y curves for cohesion component of $c-\phi$ soil (p - y) for zero, half, and full interface strength property ratios and for $b=5.5d$, $L=12\text{ m}/d=1\text{ m}$, and $\theta=30^\circ$



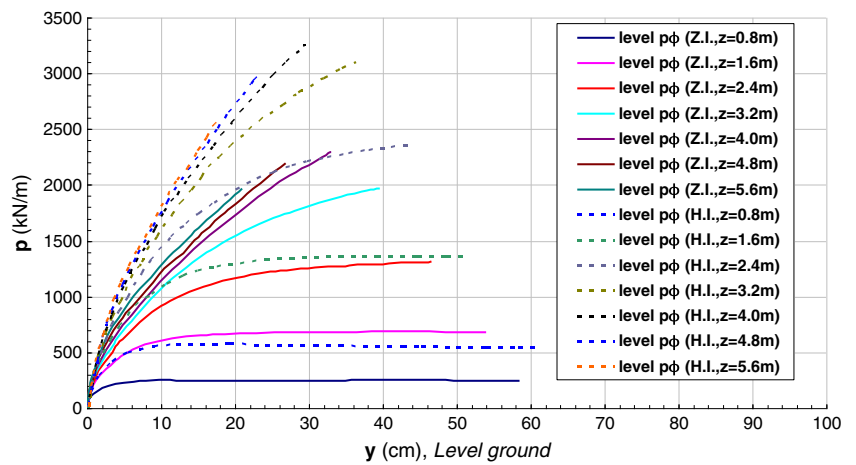
where $\Delta = \sin^{-1}(\alpha)$. For a smooth pile-soil interface ($\alpha=0$), the above equation gives $N_{pu}=9.14$, while for a semi-rough interface ($\alpha=0.5$) and fully rough interface ($\alpha=1$) gives $N_{pu}=10.82$ and $N_{pu}=11.94$, respectively.

Materials and methods

Simulation of pile lateral loading tests

Comparative results from a 3D non-linear analysis led to the conclusion that the hyperbolic approach is more appropriate for predicting the response of the mono-piles in $c-\phi$ soils similar to clayey soils (Georgiadis and Georgiadis 2010; Georgiadis and Georgiadis 2012) and rock (Liang et al. 2009). The 3D analysis consisted of a linear elastic single pile with a diameter $d=1.0\text{ m}$ and a length of $L=12.0\text{ m}$ with Poisson's ratio $\nu_p=0.1$ and Young's modulus $E_p=2.9 \times 10^7\text{ kPa}$. The soil profile consisted of sandy gravel with clay. The soil Young's modulus is $E=50\text{ MPa}$, the drained cohesion of the clayey soil is $c'=50\text{ kPa}$, and the internal frictional angle of soil is $\phi'=45^\circ$. It is pointed out that this high value of the internal friction angle is used for modeling the behavior of an artificial soil embankment consisting of $c-\phi$ soil and $\phi'=45^\circ$ is a threshold value in the analysis for all kinds of soils, and this internal friction angle

Fig. 10 Hyperbolic p - y curves for friction component of c - ϕ soil (p_{ϕ} - y), in level ground and pile-soil half interface (HI) strength property ratio and zero interface (ZI) strength property ratio for vertical concrete mono-pile with $L=12$ m/ $d=1$ m and $\theta=0^\circ$ for different depths below the ground surface ($v_{\max}=0.7d$)



shows stability for a 12 m height and 45° slope. The soil Poisson's ratio is $\nu=0.40$. The ground water table has not been considered, the unit weight of the soil is $\gamma_t=22$ kN/m³, and the coefficient of earth pressure at rest for modeling of initial stress conditions along depth z in soil profile is equal to the K_0 ; then, $\sigma_{xx}=\sigma_{yy}=K_0\sigma_{zz}$ and $\sigma_{zz}=\gamma_t z$.

The c - ϕ soil was assumed to be a linear elastic perfectly plastic material, and the elastic perfectly plastic Mohr-Coulomb constitutive model (Potts and Zdravkovic 1999; Wood 1990) has been used to simulate the behavior of the c - ϕ soil by present paper.

The normal and shear stiffness by the forms of k_n and k_s , respectively, should be defined in order to calculate the normal and shear forces in the pile-soil interface in this study, that they have (2000 Mpa/m) value in this study. Larger values for these two parameters will increase the accuracy of the calculations, but the rates of convergence time to answer will be increased as well.

The p - y curves derived from shear and normal stresses were created in interface elements due to lateral loading. Two interfaces were considered between the concrete pile and the c - ϕ soil. The first interface has a semi-cylindrical

shape and is placed between the pile walls and the c - ϕ soil, and the second interface is placed between the pile tip and the c - ϕ soil in bottom of concrete pile model. The constitutive model of the interface elements in 3D FDM is defined by a linear Coulomb shear-strength criterion that limits the shear force acting at an interface node and is given by Eq. (18)

$$F_{s\max} = c_i A + \tan\phi_i (F_n - pA) \tag{18}$$

where $F_{s\max}$ is the limiting shear force at pile-soil interface (kN), F_n is the normal force (kN), c_i is the cohesion (adhesion) between pile and soil in interface (kPa), ϕ is the internal friction angle of the interface (degree), p is the pore water pressure (kPa) (p is equal to zero in present study), and A is the contact area (m²) between pile and soil.

The triangular interface's elements connect the pile elements with the surrounding soil elements (Fig. 4). Numerical computations were speeded up, taking into account the symmetry on the vertical plane $y=0$, and thus, the half grid defined by equation $y \geq 0$ was finally considered. The other half of grid was removed, and the boundary conditions in bottom and sides of model were modified accordingly. In

Fig. 11 Hyperbolic p - y curves for friction component of c - ϕ soil (p_{ϕ} - y), in level ground and pile-soil full interface (FI) strength property ratio and zero interface (ZI) strength property ratio for concrete pile with $L=12$ m and $d=1$ m

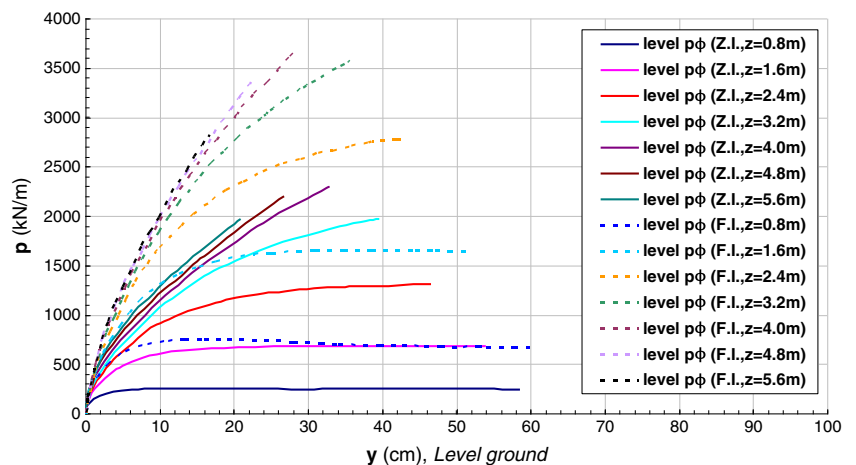
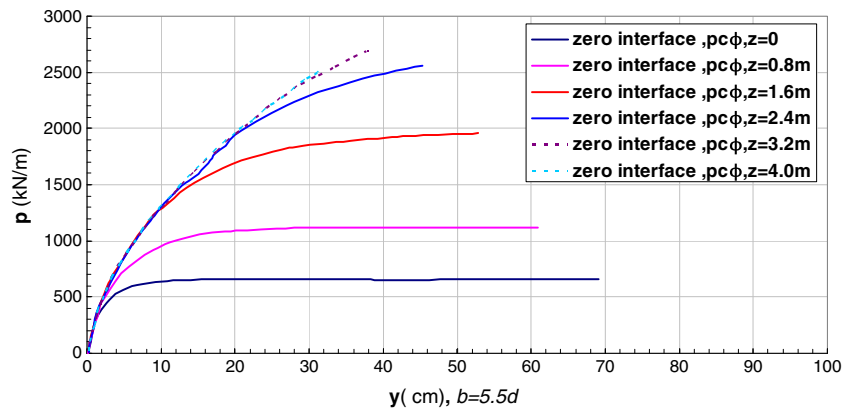


Fig. 12 Hyperbolic p - y curves for c - ϕ soil with zero interface strength property ratio, $b=5.5d$, $L=12$ m, $d=1$ m, and $\theta=30^\circ$



order to make certain that the zones and mesh size have no effect on the response of the characteristic piles, several analyses have been conducted to optimize mesh discretization and mesh density.

Parametric study

For piles under lateral loading, pile-soil interface properties have an important role in the predicted results obtained from numerical modeling. Here, the effects of pile-soil interface properties such as interface cohesion and interface friction angle on p - y curves and lateral bearing capacity of piles have been investigated. Three interface strength ratios for interface cohesion and three interfacial strength ratios for interface friction angle are considered. Therefore, the ratios that are considered for interface cohesion are $C_{int}/C_{soil}=0$, $C_{int}/C_{soil}=0.5$, and $C_{int}/C_{soil}=1.0$ for zero, half, and full pile-soil interface strength ratios, respectively, and three ratios for interface friction angle are $\tan\phi_{int}/\tan\phi_{soil}=0$ for zero strength ratio, $\tan\phi_{int}/\tan\phi_{soil}=0.5$ for half strength ratio, and $\tan\phi_{int}/\tan\phi_{soil}=1.0$ for full strength ratio.

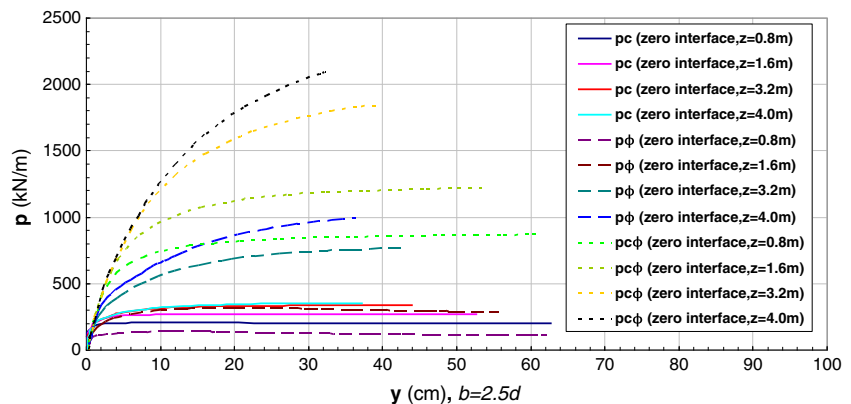
General behavior of pile-soil interface has been modeled by considering interface normal and shear stiffness. The ultimate lateral bearing capacity of the pile, p_u , in the horizontal direction is calculated by applying a horizontal velocity in positive x direction at the top of the pile head. The range of

applied velocity depended on the desired lateral pile displacement ($y_{max}=0.8d$) in x direction (Fig. 8). The velocity is applied by means of a “ramp” loading (i.e., the boundary condition at pile head is increased linearly from zero to the desired value). There is large contrast in stiffness values between the concrete or steel pile and the c - ϕ soil, which produces a large contrast in natural periods of this model. Many thousands of time steps (e.g., up to 140,000 to 1,400,000 steps for $5E-6$ (m/steps) to $5E-7$ (m/steps) loading speeds, respectively) are required to propagate a horizontal loading through the model, because the critical time step is controlled by the high stiffness of the concrete (or steel material).

Verification with available lateral load test results

In order to verify the developed method in the present study, six available tests were analyzed by present method, and then, the results were compared to the extracted load transfer curves, p - y curves, and pile-head load-deflection curves, H - y curve. In addition, Coulomb shear-strength criterion has been applied for the pile-soil interface in numerical modeling of these experiments. Also, a summary of the soil profiles and piles of these experiments was presented in Table 1. A good agreement has been observed between the experimental data and the numerical results from the present study. These tests

Fig. 13 Hyperbolic p - y curves for cohesion component of c - ϕ soil (p_c - y), p - y curves for friction component of c - ϕ soil (p_ϕ), and p - y curves for both cohesion and friction components of c - ϕ soil ($p_{c\phi}$ - y) for zero interface strength ratio conditions and for $\theta=30^\circ$, $L=12$ m, $d=1$ m, $h_{slope}=12$ m, and $y_{max}=0.7d$



are tested in cohesive soils and level ground (experiments 1 and 2), non-cohesive soil tests (experiment 3), cohesive-granular soil (experiment 4), and in cohesive soils and sloping ground (experiments 5 and 6). We remind that the experiment numbers 1 and 2 that are Sabine and Lake Austin experiments, respectively, have been performed by the Matlock (Matlock 1970) on steel pipe pile with 319 mm diameter, 12.8 m length, and wall thickness of 12.7 mm.

The average amount of strain at 50 % of soil axial strength is equal to $\epsilon_{50}=0.012$ in triaxial tests for Lake Austin test, and it is equal to $\epsilon_{50}=0.02$ for Sabine test, as well. In addition, the undrained cohesion for Sabine and Lake Austin are 14.4 and 32.25 kPa, respectively, and according to the $E_{50}=(C_u/\epsilon_{50})$ (Skempton 1951; Tomlinson 1994). E_{50} values are equal to 2060 and 2687.5 kPa for Sabine and Lake Austin tests, respectively. There are no any detailed information about resistance characteristics of the test pile-soil interfaces, but the surface adhesion coefficients are equal to $\alpha=1$ and $\alpha=0.92$ for the experiments of Sabine and Lake Austin, respectively, that are obtained from $\alpha-C_u$ graph (Georgiadis and Georgiadis 2010; Georgiadis and Georgiadis 2012; Skempton 1951; Tomlinson 1994).

In addition, the third experiment (i.e., Garston’s test) has been carried out by Price and Wardle (Price and Wardle 1987) on a bored pile (named TP15 pile) with length of 12.5 m and diameter of 1.5 m. Also, soil profile consisted of four layers of non-cohesive soil. Also, the fourth experiment has been performed by Ismael (Ismael 1990) on bored piles with length of 5 m and diameter of 0.3 m at cemented sand (i.e., $c-\phi$ soil) in Kuwait. The soil profile consists of two layers; the first layer consists of medium dense silty sand. Thereto, fifth and sixth experiments have been conducted by Bhushan et al. (Bhushan et al. 1979) on cast-in-place drilled piers for SCE Company. These two piers have diameter of 1.22 m. Furthermore, these two piers have a bell in 0.61 m (2 ft) of their ends with 1.68 m (5 ft) bottom diameter.

Fifth pier experiment (i.e., pier no. 9 in main article) (Bhushan et al. 1979) has been carried out on a pier with

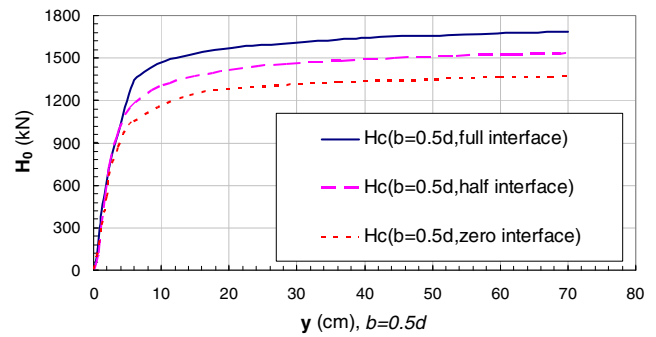


Fig. 15 Pile-head load-deflection curves for cohesion component of $c-\phi$ soil for full, half, and zero interface strength property ratios and $b=0.5d$, $\theta=30^\circ$, and $L=12\text{ m}/d=1\text{ m}$

length of 5.85 m (17 ft), in 20° slope at site C, and soil type is silty clay (CL-CH). According to the relationship of $E_{50}=(C_u/\epsilon_{50})$ (Skempton 1951; Tomlinson 1994). the $E_{50}=24.44\text{ MPa}$ for this experiment was estimated. Sixth test pier has been done on a pier (i.e., pier no. 12 in the main article) (Bhushan et al. 1979) with length of 6.71 m (22 ft) in 55° slope at site E that consisted of cemented silty sand soil (SM). The coefficient of surface adhesion α due to the high level of adhesion of these two tests (i.e., with C_u larger than 200 kPa) is equal to $\alpha=0.25$ according to the $\alpha-C_u$ graph (Georgiadis and Georgiadis 2010; Georgiadis and Georgiadis 2012; Skempton 1951; Tomlinson 1994). that it is not very precise.

Unfortunately, the main paper (Bhushan et al. 1979) has not mentioned the slope height, and this subject will cause to some differences between 3D FDA numerical model results and the experiment results, especially in the sixth experiment, due to the great height of slope. So that, the lateral pile displacement is estimated a little more than the real experiment due to the slope height and inclination conditions.

However, graphical comparisons of numerical modeling results of these six experiments have been presented by authors in Figs. 5, 6, and 7, respectively.

Fig. 14 Hyperbolic $p-y$ curves for cohesion component of $c-\phi$ soil (p_c-y), $p-y$ curves for friction component of $c-\phi$ soil (p_ϕ), and $p-y$ curves for both cohesion and friction components of $c-\phi$ soil ($p_{c\phi}$) for full interface strength ratio conditions and for $\theta=30^\circ$, $L=12\text{ m}$, $d=1\text{ m}$, $h_{\text{slope}}=12\text{ m}$, and $y_{\text{max}}=0.7d$

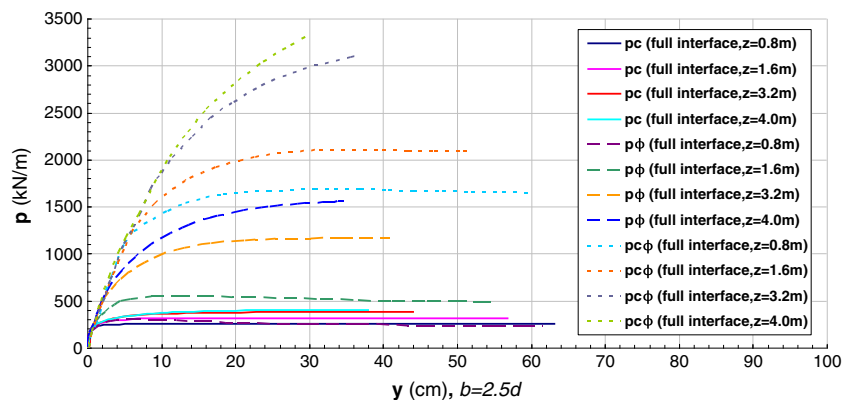
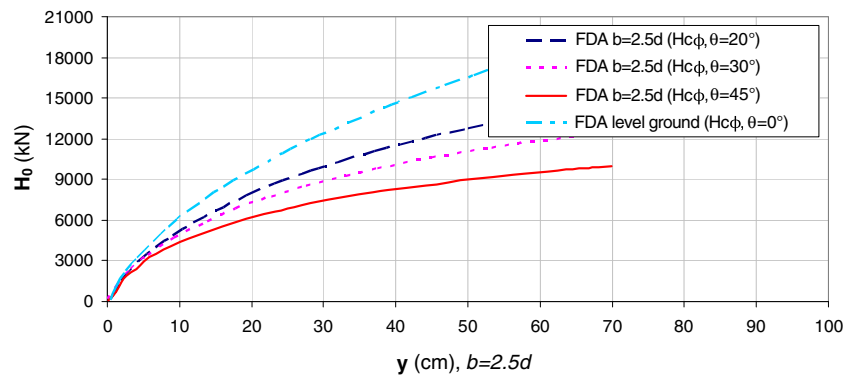


Fig. 16 Pile-head load-deflection curves for different slope inclinations for $b=2.5d$, $L=12$ m, and $d=1$ m and full interface strength property ratio in $c-\phi$ soil ($H_{c\phi}$)



Consequently, the visible discrepancies between test results and 3D FDA results can be due to the several reasons including

- (1) The effects of mathematic correlation-relationship usages,
- (2) The effects of real status of the soil and artificial numerical modeling of the soil medium,
- (3) The effects of differences between the estimated theoretical and real experimental flexural rigidity of pile and soil (i.e., $E_p I_p$ and $E_s I_s$, respectively),
- (4) The effects of dilation of the soil in the pile-soil interface and beyond of this zone,

- (5) The effects of differences in adhesion and interface internal friction angle of theoretical and real pile-soil interface,
- (6) The effects of soil aging and different behaviors of real soil slope and man-made embankment,
- (7) The effects of pile installation technique and soil disturbance around the pile,
- (8) The effects of empirical relationships and some other unknown factors.

Note that in Table 1, the e parameter means the vertical distance between the ground surface and the lateral load imposition location at pile head (i.e., loading eccentricity due to the real loading conditions and the arm of bending moment by jack loading). In addition, test results of cohesive soils have

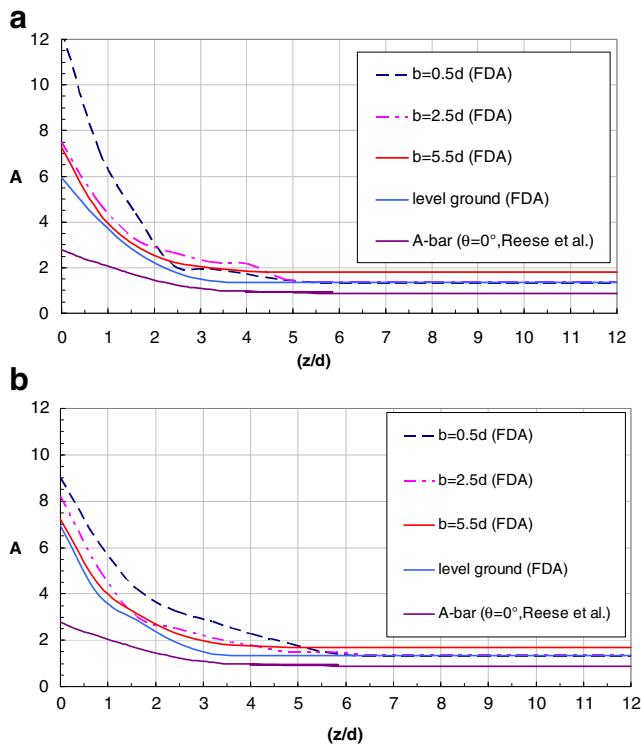


Fig. 17 Value of coefficient A for variations of z/d and b/d and for $\theta=0^\circ$ and 30° and $L=12$ m/ $d=1$ m for **a** full interface strength property ratio and **b** for half interface strength property ratio

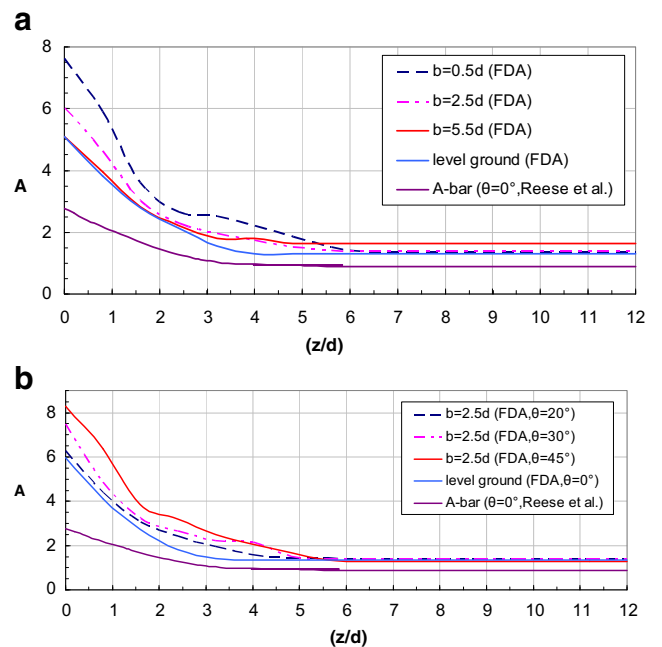


Fig. 18 Value of coefficient A for variations of z/d and b/d and for **a** zero strength interface property ratio for $\theta=0^\circ$ and 30° and $L=12$ m/ $d=1$ m and **b** for full strength interface property ratio for $\theta=0^\circ$, 20° , 30° , and 45° and $L=12$ m/ $d=1$ m

been compared with the other research results such as Matlock (Matlock 1970), Bhushan et al. (Bhushan et al. 1979), Stevens and Audibert (Stevens and Audibert 1980), O'Neill and Gazioglu (O'Neil and Gazioglu 1984), and Reese and Welch (Reese and Welch 1975).

Parametric study results and discussion

In the parametric studies, three different slope inclination angle conditions including 20, 30, and 45° have been considered. Also, three different distances between slope crest and pile cross section center including $b=0.5d$, $2.5d$, and $5.5d$ have been considered, and d is equal to concrete pile diameter and is equal to 1 m. In all the research, pile lengths are 12 m. According to the "aspect ratio" ($L/d=12$) and also relationship of K_R at Poulos (Poulos and Davis 1980), piles are in flexible type in this study and the pile heads are free against rotation (i.e., free-head pile conditions; Fig. 8). The developed p - y curves for various depths and various parametric assumptions for pile-soil interface properties have been shown in Figs. 9, 10, 11, 12, 13, and 14.

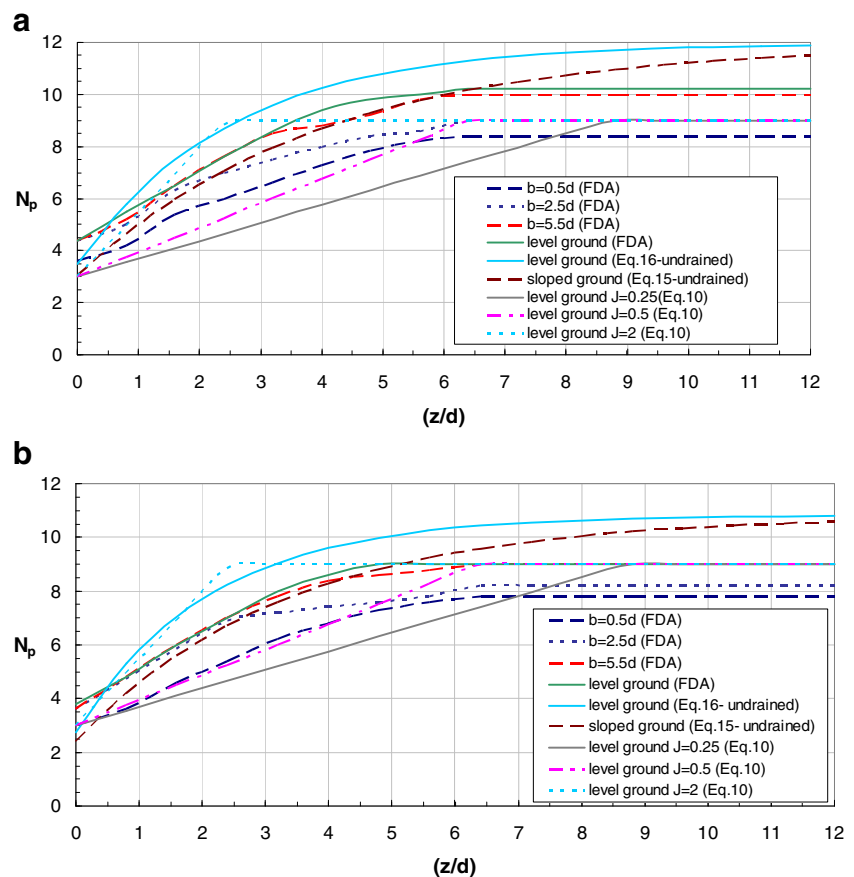
The presented p - y curves in this study are calculated according to the pile lateral displacement in different depths. First, lateral loading has been imposed on the pile head in

horizontal x direction by ramp loading, and then, mobilized shear strength of soil around the pile that has been calculated by help of normal and shear force components have been created in the pile-soil interface. The soil resistance, p , in the unit length of the pile (i.e., force/length) that is obtained by calculation of the forces has been generated in the pile-soil interface; therefore, the p - y curves are depicted by having the rate of corresponding lateral displacements of piles, as shown in Figs. 8, 9, 10, 11, 12, 13, and 14.

As shown in Figs. 9, 10, 11, 12, 13, and 14, the strength properties of the pile-soil interface have a great effect on the soil strength estimation (i.e., estimation of p) and changing the p - y curve shape. In some cases, there are more than 50 % changes in p - y curve values by increasing the pile-soil interface strength properties, such as cohesion and internal friction angle of the interface area, according to the Coulomb shear-strength criterion. As seen in these figures, the final values of p_u and also their p values, for both cohesion component and friction component, are strongly influenced by the strength properties defined by the pile-soil interface properties, and by increasing these properties, the p value will be increased, as well. Figures 15 and 16 show the load-deflection curves for pile heads (i.e., H - y curves).

Figure 15 shows the H - y curves for cohesion component of the c - ϕ soil alone, and Fig. 16 shows H - y curves for both

Fig. 19 Variation of lateral bearing capacity factor N_p with b/d and z/d for **a** full interface strength property ratio and **b** half interface strength property ratio for $\theta=0^\circ$ and 30° and $L=12$ m and $d=1$ m



cohesion and friction components of $c-\phi$ soil for different slope inclination angles. Also, variations in values of pile-head lateral load bearing capacity, H , and pile-head deflection, y (i.e., H - y curves), are affected by strength properties defined by the pile-soil interface properties similar to p - y curves. As shown in Fig. 16, by reducing the slope inclination angle, the amounts of the pile-head loads have been increased, and according to the results of 3D FDA by increasing the distance between slope crest and pile center, the ultimate strength of the soil has increased and more pile-head lateral load bearing capacity (i.e., H component) is calculated.

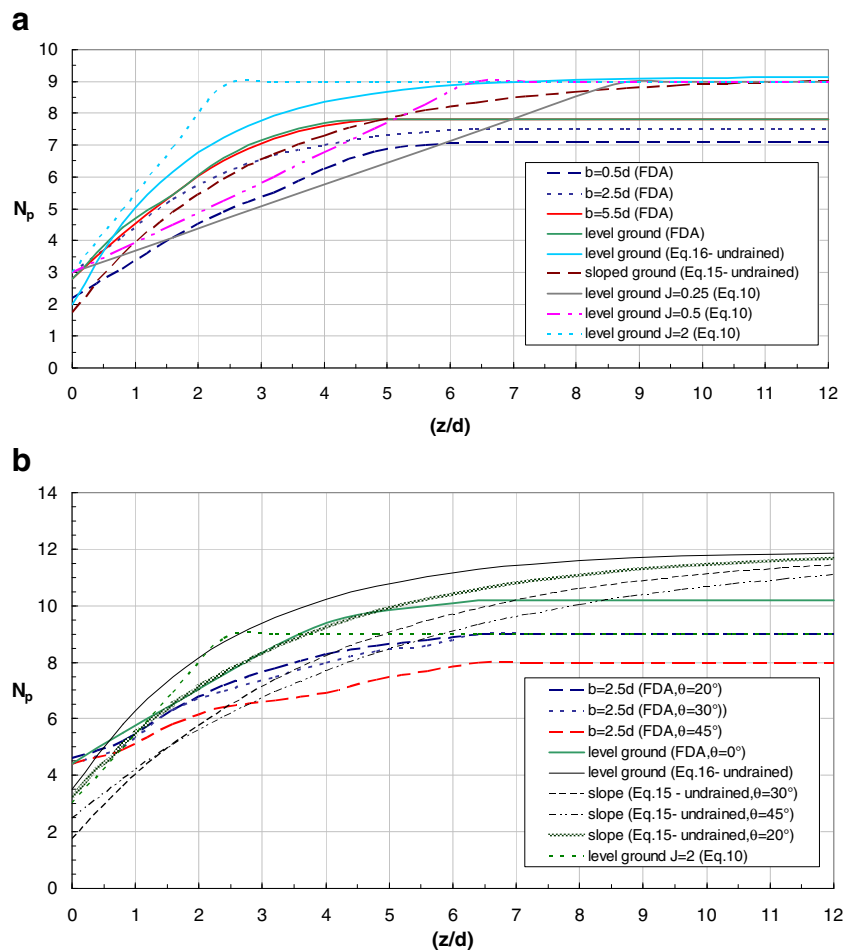
According to Figs. 17 and 18, the A coefficient values have been calculated and have already been presented according to Eq. (14) based on the dimensionless depth (Z/d) for different interfacial strength ratios. By using this value, we can create the last relationship (i.e., Eq. (13)) between the components of soil ultimate strength that are resulted by cohesion component (i.e., p_{ultc}) and friction component, (i.e., $p_{ult\phi}$), and the ultimate strength of the soil is resulted by effects of both cohesion and friction components (i.e., $p_{ultc\phi}$), according to Eqs. (7) and (13).

Moreover, according to these equations, the value of this coefficient (i.e., A coefficient) is decreased by increasing the

distance between slope crest and pile-head center. Although some scattering that have been caused by numerical errors can be seen, the overall shapes of the curves reflect this fact that the coefficients of A will be decreased by increasing the distance between the slope crest and the pile-head center. Figure 18b shows that increasing the slope angle will increase the coefficient A and both these results mean that the frictional component of $c-\phi$ soil will more participate in overall bearing capacity of $c-\phi$ soil by increasing the distance of pile center to slope crest and also by reducing the slope inclination angle.

The coefficient of lateral bearing capacity, N_p , in the drained cohesion component of $c-\phi$ soil is resulted by 3D FDA, for different strength ratios in pile-soil interface properties that have been mentioned in “Parametric study” section are displayed in Figs. 19 and 20. N_p-z/d equations were calculated by refs. Georgiadis and Georgiadis (2010) and Georgiadis and Georgiadis (2012) despite taking into account the slope inclination angle, surface adhesion, the pile-soil interface properties, and depth z cannot able to take the effect of (b/d), distance ratio, on the N_p values, into account. It seems better to present some graphs to modify an equation to taking into account the effect of (b/d) ratios (Georgiadis and Georgiadis 2010; Georgiadis and Georgiadis 2012).

Fig. 20 Variation of N_p with z/d and dimensionless distance b/d for **a** zero interface strength property ratio for $\theta=0^\circ$ and 30° and $L=12$ m and $d=1$ m and **b** full interface strength property ratio and different θ for $b=2.5d$, $L=12$ m, and $d=1$ m



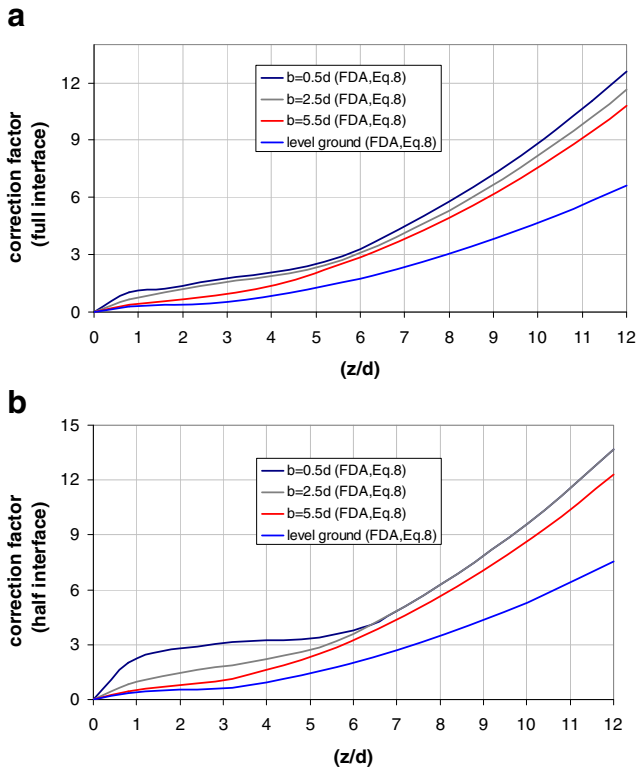


Fig. 21 Correction factor graphs for Eq. (8) and for **a** full interface strength ratio and **b** half interface strength ratio for $L=12$ m, $d=1$ m, and $\theta=0^\circ$ and 30°

However, several graphs are presented in Figs. 21, 22, 23, and 24 in order to correct the derived values from

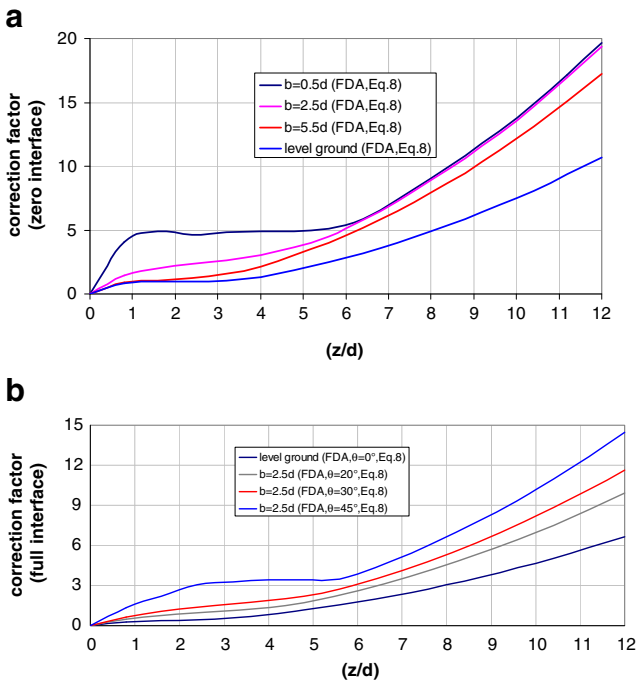


Fig. 22 Correction factor graphs for Eq. (8) for **a** zero interface strength ratio for $\theta=0^\circ$ and 30° and **b** full interface strength ratio and different slope inclination angles for $b=2.5d$, $L=12$ m, and $d=1$ m

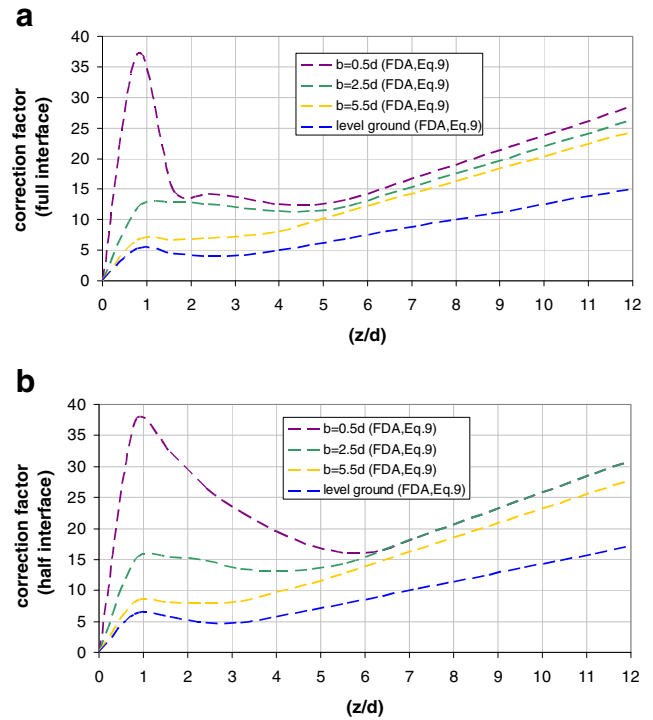


Fig. 23 Correction factor graphs for Eq. (9) and for **a** full interface strength ratio for $\theta=0^\circ$ and 30° and **b** half interface strength ratio for $L=12$ m/ $d=1$ m, $\theta=0^\circ$ and 30° , $b=0.5, 2.5$, and $5.5d$, and level ground ($b/d=\infty$)

Eqs. (8) and (9) to the frictional resistance component of the $c-\phi$ soil (i.e., $p_{ult\phi}$). The amounts of Eq. (8) were divided by the 3D FDA values in graphs of Figs. 21 and

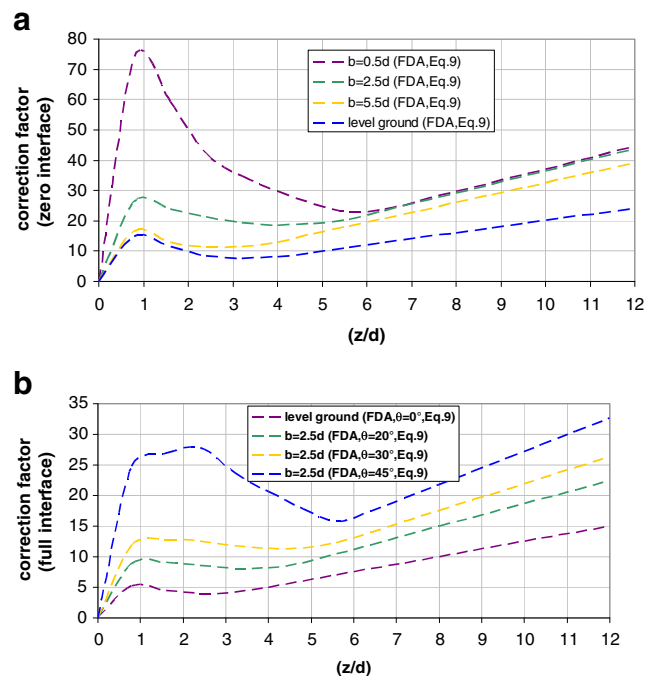


Fig. 24 Correction factor graphs for Eq. (9) and for **a** zero interface strength ratio for $\theta=30^\circ$ and **b** full interface strength ratio and different slope inclination angles for $L=12$ m/ $d=1$ m and $b=2.5d$

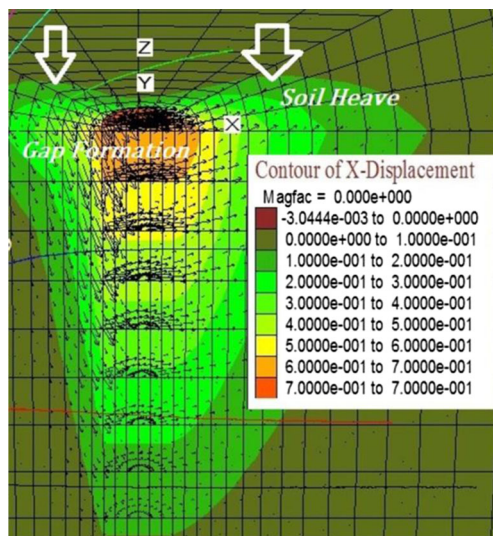


Fig. 25 Gap formation in rear of pile head and soil heave in front of pile head, during lateral loading

22, so to obtain the resulted value derived from 3D FDA method, we should divide the Eq. (8) values by the 3D FDA obtained graph values. Similarly, this process was recurred for Eq. (9), in graphs of Figs. 23 and 24, by the difference that it is due to the existence of terms $\tan^4\beta$ and in particular the term of $\tan^8\beta$; it has created large coefficients in Figs. 23, 24, and 25.

Conclusions and discussions

The effects of cohesion and angle of internal friction components and pile-soil interfacial strength properties for concrete mono-pile adjacent soil slopes and also in level ground by 3D FDA were examined in the present study. These investigations have a special attention to the study of strength properties of pile-soil interface. This study examines the cohesion and internal friction effects on bearing capacity of piles under lateral loading in drained mixed c - ϕ soils. The results of the pile-soil interface strength property effects in estimating the ultimate lateral bearing capacity of piles under static lateral loading in sloped and level grounds are investigated in this study. The main results of present study can be summarized as follows:

1. Pile's head have no displacement, where the p - y curves reach to their ultimate value (i.e., the horizontal line in p - y curves) along the pile length. In fact, the p - y curves of all depths do not reach to their final p_u in a specified displacement y_0 on pile head and do not have a similar shape. However, as observed in the actual curves of the static lateral load test results, the p - y curves reach to their ultimate amount p_u in shallow depths. It can be considered the amount of p in that depth as the ultimate p_u for that appropriate pile-head displacement. These assumptions

are close to the pile-head displacement behaviors in reality.

2. The effects of cohesion and friction angles of pile-soil interface were studied in details in this paper, and it was understood that these two factors are most influential factors on static lateral load transfer behavior of pile (i.e., p - y curve behavior) and accurate selection of these two parameters in numerical simulations can influence the results, estimating the pile-soil behavior. It should be noted that in this study, the effects of soil dilation angle and pile-soil interfacial dilation during lateral loading are ignored, whereas these two factors can have an important role in approaching real behavior of pile-soil system during numerical simulations. Therefore, studying the effects of these two factors could be an important future research topic.
3. During static lateral loading in a practical experiment, the soil in rear of the pile-head face with gap formation (i.e., cracking behavior) and the soil in front of pile-head face with soil heave (i.e., swelling behavior) and both of these two events in 3D FDA have been observed through the displacement vectors. However, these phenomena are completely in agreement with the practical results of recent experiments (Nimityongskul and Ashford 2010; Nimityongskul et al. 2012).
4. By using elastic-perfect plastic models, such as Tresca (Georgiadis and Georgiadis 2010; Georgiadis and Georgiadis 2012) and Mohr-Coulomb models, the p - y curve shapes for any kinds of soils including cohesive soils (drained or undrained), granular soils, and mixed cohesive-granular soils (i.e., the c - ϕ soils and subject of this paper) are hyperbolic similar to resulted curve shapes by present study. However, this phenomenon is due to the lack of considering softening and hardening behaviors in the aforesaid models that ignored softening/hardening behaviors during gap and crack formations, in the soil under lateral loading in rear and front of the pile head, respectively.
5. According to the results of our numerical study, the p - y curve starts in the depth of $z=0$ (i.e., at the ground surface level) in cohesive soils, due to their nature. It should be noted that this phenomenon is consistent with the theoretical results and current experiments. But in granular soils, there is no any p - y curve formation in depth of $z=0$ that is consistent with theoretical results and current experiments, as well.
6. According to the A - (z/d) graphs that have been derived from 3D FDA in this study, the frictional component of c - ϕ soil will have more participation in overall lateral loading capacity of c - ϕ soil by decreasing the slope inclination angle and by increasing the distance between pile center and slope crest, whereas inverse process of this situation is visible for the cohesion component of c - ϕ soil.

References

- American Petroleum Institute, API (1987) Recommended practice for planning, designing, and constructing fixed offshore platforms. API Recommended Practice 2A (RP-2A), 17th edition
- Bhushan K, Haley SC, Fong PT (1979) Lateral load tests on drilled piers in stiff clays. *J Geotech Eng Div ASCE* 105(8):969–985
- Comodromos EM, Papadopoulou MC (2010) On the response prediction of laterally loaded fixed-head pile groups in sands. *J Comput Geotech* 37:903–941
- Comodromos EM, Papadopoulou MC (2013) Explicit extension of the p-y method to pile groups in cohesive soils. *J Comput Geotech* 47:28–41
- Evans LT, Jr, Duncan JM (1982) Simplified analysis of laterally loaded piles. report UCB/GT/82-04, University of California, Berkeley
- Gabr MA, Borden RH (1990) Lateral analysis of piers constructed on slopes. *J Geotech Eng* 116(12):1831–1850
- Georgiadis K, Georgiadis M (2010) Un-drained lateral pile response in sloping ground. *J Geotech Geoenviron Eng ASCE* 136(11):1489–1500
- Georgiadis K, Georgiadis M (2012) Development of p-y curves for un-drained response of piles near slopes. *Comput Geotech* 40:53–61
- Georgiadis M, Anagnostopoulos C, Safflekou S (1991) Interaction of laterally loaded piles. *Proceedings Fondations Profondes, Ponts et Chaussees, Paris*, pp177–84
- Ismael NF (1990) Behavior of laterally loaded bored piles in cemented sands. *J Geotech Eng, ASCE* 116(11):1678–1699
- Kim BT, Kim NK, Lee WJ, Kim YS (2004) Experimental load-transfer curves of laterally loaded piles in Nak-Dong River sand. *J Geotech Geoenviron Eng* 130(4):416–425
- Lesny K, Paikowsky SG, Gurbuz A (2007) Scale effects in lateral load response of large diameter mono-piles. *Contemporary issues in deep foundations. GSP 158. Denver, Colorado*
- Liang R, Yang K, Nusairat J (2009) P-Y criteria for rock mass. *J Geotech Geoenviron Eng* 135(1):26–36
- Matlock H (1970) Correlations for design of laterally loaded piles in soft clay. In: *Proceedings of the 2nd Annual Offshore Technology Conference. Houston*; pp 577–94 [OTC 1204]
- Mezazigh S, Levacher D (1998) Laterally loaded piles in sand: slope effect on p-y reaction curves. *J Can Geotech J* 35(3):433–441
- Murff JD, Hamilton JM (1993) P-ultimate for undrained analysis of laterally loaded piles. *J Geotech Eng* 119(1):91–107
- Muthukkumaran K, Sundaravadevelu R, Ganghi SR (2008) Effects of slope on p-y curves due to surcharge load. *J Soil Found* 48(3): 353–361
- Nimityongskul N, Ashford S (2010) Effect of soil slope on lateral capacity of piles in cohesive soils. In: *Proceedings 9th US national and 10th Canadian conference on earthquake engineering, Toronto*; [paper no. 366]
- Nimityongskul N, Barker P, Ashford SA (2012) Effects of soil slope on lateral capacity of piles in cohesive and cohesion-less soils. Final report of a research project funded by Caltrans under facilities contract No. 59A0645; The Kiewit center for infrastructure and transportation, Oregon state university; March 2012; USA
- Norris GM (1986) Theoretically based BEF laterally loaded pile analysis. *Proceedings of the 3th International Conference on Numerical Methods in Offshore Piling. TECHNIP ed.* pp 361–86
- O’Neil MW, Gazioglu SM (1984) An evaluation of p-y relationships in clays. Report Prepared for the American Petroleum Institute, University of Houston, Texas
- Ortigao JA (1995) Soil mechanics in the light of critical state theories. Balkema, Rotterdam
- Potts DM, Zdravkovic L (1999) Finite element analysis in geotechnical engineering, Theory. Vol. 1.1st ed. Thomas Telford, London
- Poulos HG, Davis EH (1980) Pile foundation analysis and design. John Wiley & Sons Ltd., New York
- Price G, Wardle IF (1987) Lateral load tests on large diameter bored piles. Contractor report: Transport and road research laboratory, Department of transport, Crowthorne; Berkshire, England; pp 45–46
- Rajashree SS, Sitharam TG (2001) Non-linear finite element modeling of batter piles under lateral load. *J Geotech Geoenviron Eng* 127(7): 604–612
- Randolph MF, Houlsby GT (1984) The limiting pressure on a circular pile loaded laterally in cohesive soil. *J Geotechnique* 34(4):613–623
- Reese LC, Van Impe WF (2001) Single piles and pile group under lateral loading. A. A. Balkema, Rotterdam, p 463
- Reese LC, Van Impe WF (2007) Single piles and pile group under lateral loading. A. A. Balkema publishers, Rotterdam
- Reese LC, Welch RC (1975) Lateral loading of deep foundations in stiff clay. *J Geotech Eng Div ASCE* 101(7):633–649
- Reese LC, Cox WR, Koop FD (1974) Analyses of laterally loaded piles in sand. In: *Proceedings of the 6th offshore technology conference. Houston*; pp 473–85 [OTC 2080]
- Reese LC, Cox WR, Koop FD (1975) Field testing and analysis of laterally loaded piles in stiff clay. In: *Proceedings of the 7th offshore technology conference. Houston*; pp 671–90 [OTC 2312]
- Skempton AW (1951) The bearing capacity of clays. *Proc Bulding Research Congress, Division 1, London: England*; pp 180–88
- Stevens JB, Audibert JME (1980) Re-examination of p-y curve formulation. *Proceedings of 11th Offshore Technology Conference, OTC, Houston*, pp 397–403, [OTC 3402]
- Tomlinson MJ (1994) Pile design and construction practice, 4th edn. E&FN SPON, London
- Welch RC, Reese LC (1972) Laterally loaded behavior of drilled shafts. Research report 3-5-65-89; Center for highway research; University of Texas, Austin
- Wood DM (1990) Soil behavior and critical state soil mechanics. Cambridge University Press, London
- Wu D, Broms BB, Choa V (1998) Design of laterally loaded piles in cohesive soils using p-y curves. *J Soils Found* 38(2):17–26
- Zhang LM, Ng CWW, Lee CJ (2004) Effects of slope and sleeving on the behavior of laterally loaded piles. *J Soil Found* 44(4):99–108